

Electrical conductivity and activation volume of the solid electrolyte phase α -AgI and the high-pressure phase fcc AgI

B.-E. Mellander*

Chalmers University of Technology, Department of Physics, S-412 96 Göteborg, Sweden

(Received 21 June 1982)

The α phase of silver iodide which is stable between 147 and 555 °C at normal pressure is a classical example of a solid electrolyte. In this investigation the temperature and pressure dependences of the electrical conductivity in α -AgI have been studied for pressures up to 0.9 GPa. This phase is characterized by a large electrical conductivity, a low migration enthalpy of 0.098 eV, and a low activation volume of 0.8–0.9 cm³ mole⁻¹. For pressures between 0.4 and 10 GPa a rocksalt-structure phase fcc AgI is stable at room temperature. The temperature and pressure dependences of the electrical conductivity in this phase have been studied for pressures up to 1.0 GPa and for temperatures between room temperature and 330 °C. The electrical conductivity resembles that in AgCl and AgBr, and it is indicated that Frenkel defects dominate also in fcc AgI. At high temperature and pressure, however, a gradual increase of the electrical conductivity takes place in fcc AgI, similar to the gradual transitions that have been reported for many materials with the fluorite structure. The electrical conductivity in this temperature and pressure range of fcc AgI is approximately 1 $\Omega^{-1}\text{cm}^{-1}$, i.e., only slightly less than the electrical conductivity in the α phase.

I. INTRODUCTION

The α phase of silver iodide, which is stable between 147 and 555 °C at normal pressure, is a typical example of a solid electrolyte.^{1–5} As early as 1914, Tubandt and Lorenz⁶ found that the electrical conductivity in this solid is as high as that for a molten salt, ranging from 1.3 to 2.6 $\Omega^{-1}\text{cm}^{-1}$ over a temperature interval of 400 K. The structure of α -AgI was first studied by Strock,⁷ who found that the iodide ions form a bcc lattice (space group *Im3m*). Strock suggested that the silver ions were distributed over 42 crystallographic sites: 6 (*b*) octahedral, 12 (*d*) tetrahedral, and 24 (*h*) trigonal. During the last few years, several studies have been performed in order to determine the silver positions in the lattice. X-ray and neutron diffraction,^{8–10} as well as extended x-ray-absorption fine-structure investigations,^{11–13} have shown that the silver ions are distributed over the tetrahedral sites while the octahedral sites are not occupied. Thus each silver ion has six equivalent sites available. This silver distribution was also suggested from Raman studies.¹⁴ The motion of the silver ions between the tetrahedral sites has been shown to occur in the $\langle 110 \rangle$ direction, i.e., via the trigonal sites.^{8,9,11,13} These results are also supported by molecular-dynamics simulations.^{15,16}

At room temperature and normal pressure two

phases exist in silver iodide, the β phase (wurtzite structure) and the γ phase (sphalerite structure), where the latter is claimed to be metastable.^{17–19} Both these phases have some unusual properties, e.g., a negative thermal-expansion coefficient.^{17,20,21} At high pressure, an intermediate phase is stable within a narrow temperature and pressure range,^{22,23} but more interesting is the rocksalt-structure phase fcc AgI, which is stable for pressures between 0.38 and 10 GPa at room temperature,^{24–30} since this phase has the same structure as that of AgCl and AgBr at normal pressure. The phase diagram for AgI for pressures up to 1 GPa is shown in Fig. 1.

Measurements of the temperature and pressure dependence of the electrical conductivity can serve as a useful tool in the study of ion transport in ionic crystals if the electronic contribution to the conductivity is negligible. For electrical conductivity σ due solely to the presence of thermally activated defects,^{31–34}

$$\sigma T = (\sigma T)_0 \exp\left[-\left(\frac{1}{2}\Delta H_f + \Delta H_m\right)/kT\right], \quad (1)$$

where T is the absolute temperature, ΔH_f and ΔH_m are the formation and migration enthalpies for the fundamental defects which permit ionic motion (usually Frenkel or Schottky defects), and k is the Boltzmann constant. The preexponential factor $(\sigma T)_0$ is, e.g., for Frenkel defects,

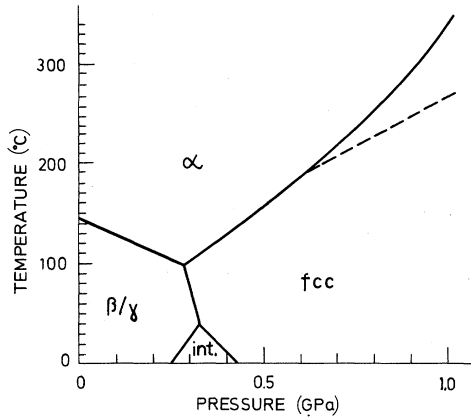


FIG. 1. Phase diagram of AgI (Ref. 22). The dashed line indicates the approximate position of the knee in the conductivity curves separating regions I' and I'' in the fcc phase.

$$(\sigma T)_0 = \frac{q^2 a^2 \alpha \nu N^{1/2} M^{1/2}}{k} \exp \left[\frac{\Delta S_f}{2k} + \frac{\Delta S_m}{k} \right], \quad (2)$$

where q is the ion charge, a the jump distance, α a geometrical factor, and ν the jump-attempt frequency. N and M are the number of lattice sites and interstitial sites per unit volume, and ΔS_f and ΔS_m are the formation and migration entropies for the defect. The temperature range where Eqs. (1) and (2) are valid is called the intrinsic temperature range. At lower temperatures, the defects caused by the presence of aliovalent impurities dominate instead, and in this temperature region, the extrinsic region, we get

$$\sigma T = (\sigma T)_0 \exp(-\Delta H_m/kT). \quad (3)$$

The formation and migration volumes for defects are defined through

$$(\partial \Delta G_f / \partial p)_T = \Delta V_f, \quad (4)$$

$$(\partial \Delta G_m / \partial p)_T = \Delta V_m, \quad (5)$$

where ΔG_f and ΔG_m are the Gibbs free energies for formation and migration of a defect. It can be shown that for an ionic conductor the activation volume ΔV can be written as³⁵

$$\Delta V = \Delta V_f / 2 + \Delta V_m = kT \left[\frac{\partial}{\partial p} \ln R \right]_T + \kappa \gamma, \quad (6)$$

where R is the electrical resistance of the sample, κ the isothermal compressibility, and γ the Grüneisen parameter. Equation (6) is valid in the intrinsic temperature range; for the extrinsic range, we get

$$\Delta V = \Delta V_m = kT \left[\frac{\partial}{\partial p} \ln R \right]_T + \kappa \gamma. \quad (7)$$

Typical for the crystal structure of a solid electrolyte is that the immobile ions form a regular space lattice, while the mobile ions are distributed over many available sites. The mobile ions have only to surmount a low energy barrier to get from one site to another, and the sites are interconnected to allow, in many cases, transport in three dimensions. The high electrical conductivity is thus due not to a large number of thermally activated Frenkel or Schottky defects, but to an inherent property of the lattice. The number of available sites is not temperature dependent, and thus for a solid electrolyte Eqs. (3) and (7) also describe the electrical conductivity at high temperatures. In this paper the pressure and temperature dependences of the electrical conductivity for the solid electrolyte α -AgI and for the high-pressure-phase fcc AgI are reported for the pressure range up to 1 GPa.

II. EXPERIMENTAL

A two-step high-pressure apparatus (Basset-Bretagne-Loire, Sevres, France) was used in this work. The pressure-transmitting medium was argon gas and the maximum pressure 1 GPa (10 kbar). A liquid-nitrogen trap and a hot trap were used between the first- and second-pressure step to remove contamination from the gas. The pressure cell was externally heated, and, in some cases, a small internal heater was used to supplement the main external heater. A Manganin pressure gauge (Somelec, Paris, France) was used to measure the pressure to $\pm 1\%$.

Polycrystalline pellets of AgI were used, since single crystals are likely to break in the first-order transitions to the α or fcc phases. The AgI powder was pressed in cylindrical dies of 15- or 8-mm diameter using a pelletizing pressure of 200–400 MPa. Two types of pellets were made. Both had two electrodes consisting of a silver-wire helix immersed in a mixture of silver iodide and silver powder, see Fig. 2. The first type of sample had a silver iodide layer of about 6-mm thickness between the electrodes. The second type of sample had two additional silver-wire electrodes inside the silver iodide layer. The central silver electrodes served as potential terminals in four wire measurements, and the mixed silver–silver-iodide electrodes served as the current terminals. This type of sample was used for measurements in the α phase and for some mea-

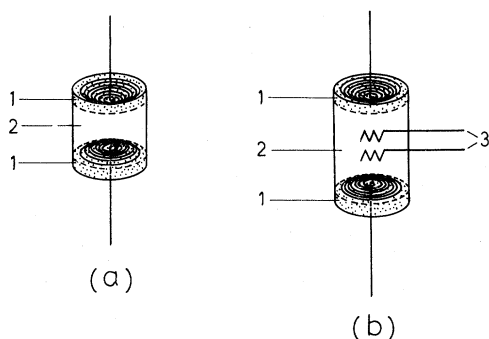


FIG. 2. (a) Two-electrode sample and (b) four-electrode sample. 1—Electrode of mixed silver and silver iodide. 2—Pure silver iodide. 3—Potential electrodes for four-wire measurements.

measurements at high temperature in the fcc phase. No difference could, however, be detected in the results using two or four electrode samples. In the α phase the resistance of the samples was very low, typically 0.2Ω for the four-electrode pellets.

The silver iodide used for the measurements in the α phase was stated to be better than 98% pure (KEBO AB, Stockholm, Sweden) or precipitated from potassium iodide and silver nitrate,³⁶ where both constituents were of analytical quality (E. Merck, Darmstadt, Germany). The silver iodide used for most measurements in the fcc phase was stated to be 99.9% pure (Riedel-deHaën, Hanover, Germany). The electrical resistance of the two-electrode samples was measured by either a Radiometer GB 11a impedance bridge or a Hewlett-Packard 4261A LCR meter. With the use of the impedance bridge the frequency range 25 Hz–100 kHz could be investigated. In order to determine the resistance of the samples complex impedance plots were used.³⁷ Since the samples had nonblocking electrodes, the electrical conductivity was not frequency dependent at low frequencies, and the resistance measured at 1 kHz was used for most samples.

The four-electrode samples had the current terminals connected in series with a standard resistor and a frequency generator. The voltages across the potential electrodes and the standard resistor were measured by a Solartron A203 digital voltmeter connected to a Solartron data transfer unit. In this case a frequency of 1 kHz could also be used for most samples. Since the samples did not have well-defined boundaries between the electrodes and the electrolyte, it was difficult to determine the cell constant accurately. The cell constant is, however, important only for the determination of the prefac-

tor $(\sigma T)_0$. The accuracy of the resistance measurements was $\pm 1\%$.

The temperature was measured by a Chromel-Alumel thermocouple placed close to the sample. No correction for the effect of pressure on the thermoelectric power was applied since earlier investigations^{38–40} show that this effect is small for Chromel-Alumel thermocouples, at least for temperatures below 450°C .⁴⁰ The accuracy of the temperature measurements is estimated to be better than ± 2 K.

III. RESULTS

A. α -AgI

The temperature and pressure dependences of the electrical conductivity were investigated for temperatures up to 350°C using a maximum pressure of 0.9 GPa. For the constant pressure runs, the measured electrical conductivity was plotted in $\ln(\sigma T)$ vs $1/T$ diagrams, and the points were least-squares fitted to a straight line. The migration enthalpy could then be determined from Eq. (3). In Fig. 3 the electrical conductivity is shown for a constant pressure run at 0.27 GPa, which is close to the region where the maximum temperature range could be obtained.

Very good agreement with a straight line was obtained and the migration enthalpy, for pressures below 0.5 GPa, was found to be independent of

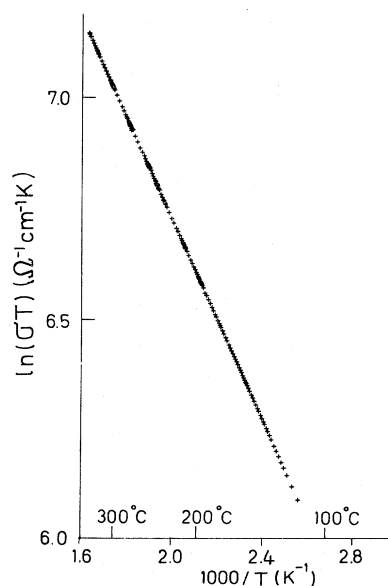


FIG. 3. $\ln(\sigma T)$ vs $1/T$ for α -AgI at 0.27 GPa.

pressure, with a mean value of 0.098 ± 0.001 eV. The mean value for the prefactor $(\sigma T)_0$ was $(8.0 \pm 0.3) 10^3 \text{ K } \Omega^{-1} \text{ cm}^{-1}$. The errors given here are the standard deviation of the mean.

The electrical conductivity decreases with increasing pressure, but only by about 1% for a pressure difference of 0.1 GPa. In Fig. 4 some examples of $\ln(1/R)$ versus pressure plots are shown. Straight lines were least-squares fitted to the measured values, and the migration volume was determined from Eq. (7). The only compressibility study known to us for α -AgI (Ref. 41) gives $\kappa = 5.56 \times 10^{-11} \text{ m}^2/\text{N}$ and the Grüneisen parameter γ was calculated using

$$\gamma = V_m \beta B / C_V, \quad (8)$$

where V_m is the molar volume, β the volume thermal-expansion coefficient, B the bulk modulus, and C_V the molar specific heat at constant volume. C_V was, in turn, calculated using

$$C_V = C_P - TV_m \beta^2 / \kappa. \quad (9)$$

The molar specific heat at constant pressure C_P for α -AgI has been much discussed in the literature.^{36,42,43} In the present study the value⁴⁴ $C_P = 57.2 \text{ J mole}^{-1} \text{ K}^{-1}$ was used, and together with the values^{17,45,46} $V_m = 39.9 \text{ cm}^3 \text{ mole}^{-1}$, $\beta = 9.3 \cdot 10^{-5} \text{ K}^{-1}$, and the compressibility value given above,⁴¹ we get $C_V = 54 \text{ J mole}^{-1} \text{ K}^{-1}$ at 500 K. The Grüneisen constant could then be calculated from Eq. (8), since $B = 1/\kappa$, which gives $\gamma = 1.24$. This value is somewhat lower than that for "normal ionic crystals," where a typical value is 1.4–2.0. The migration volumes calculated using

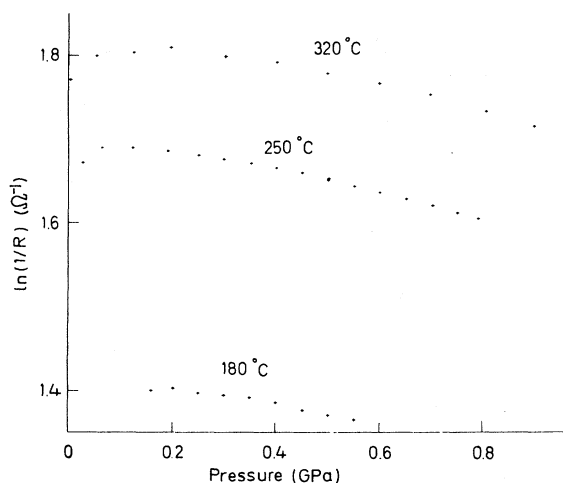


FIG. 4. Pressure dependence of $\ln(1/R)$ for three α -AgI samples.

these data are summarized in Table I, together with the results of Allen and Lazarus.⁴⁷ For pressures below about 0.15 GPa, an increase of the electrical conductivity could be seen in some experiments. Since this could be due to the difficulties to obtain a constant temperature in the pressure range below 0.15 GPa with the present equipment, the measured points for pressures below 0.15 GPa were not included in the least-squares fit. The same practice was followed by Allen and Lazarus,⁴⁷ who ignored points below 0.1 GPa. Table I(a) shows that $kT\kappa\gamma$ is comparable in size to $kT\partial(\ln R)/\partial p$. The accuracy of the migration volumes are thus strongly dependent on the accuracy of $\kappa\gamma$. The total error in the ΔV_m values is estimated to be about $\pm 0.1 \text{ cm}^3 \text{ mole}^{-1}$.

B. fcc AgI

The rocksalt-structure phase fcc AgI was investigated in the pressure range 0.48–1.0 GPa and in the temperature range from room temperature up to 330 °C. The temperature dependence of the electrical conductivity was studied at six different pressures between 0.48 and 1.0 GPa. The largest temperature interval, more than 300 K, was covered in the 0.9-GPa run. The $\ln(\sigma T)$ vs $1/T$ plots for some of the runs are shown in Fig. 5. The formation enthalpy ΔH_f and the migration enthalpy ΔH_m can be determined using Eqs. (1) and (3), if the transport mechanism is assumed to be the same in both ranges. These enthalpies might be obtained by fitting straight lines to the high- and low-temperature parts of the conductivity plot. This procedure re-

TABLE I. (a) Results for the constant temperature measurements in α -AgI. (b) The migration volume of α -AgI according to Allen and Lazarus (Ref. 47).

Temperature (°C)	$kT\partial(\ln R)/\partial p$ ($\text{cm}^3 \text{ mole}^{-1}$)	$kT\kappa\gamma$ ($\text{cm}^3 \text{ mole}^{-1}$)	ΔV_m ($\text{cm}^3 \text{ mole}^{-1}$)
(a)			
187	0.51	0.26	0.77 ± 0.1
250	0.55	0.30	0.85 ± 0.1
320	0.58	0.34	0.92 ± 0.1
Tempertaure (°C)	ΔV_m ($\text{cm}^3 \text{ mole}^{-1}$)		
(b)			
162	0.56 ± 0.1		
228	0.65 ± 0.1		
283	0.5 ± 0.1		
350	0.8 ± 0.1		

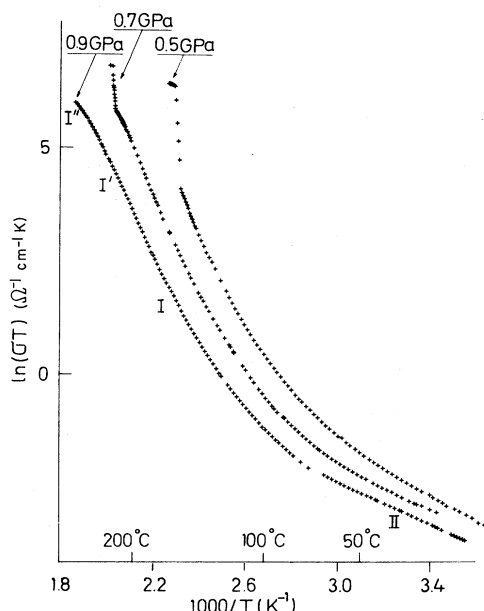


FIG. 5. Temperature dependence of the electrical conductivity of fcc AgI at 0.5, 0.7, and 0.9 GPa. The sudden increase in conductivity for the 0.5 and 0.7 GPa runs corresponds to the transition to the α -phase.

quires that the straight regions of the conductivity curve are extended over wide temperature ranges. From Fig. 5 we can see that this is not the case for fcc AgI. In the present work, the measured points were, instead, least-squares fitted to a sum of two exponentials

$$\sigma T = a_I \exp(-\Delta E_I/kT) + a_{II} \exp(-\Delta E_{II}/kT) \quad (10)$$

by changing the parameters a_I , a_{II} , ΔE_I , and ΔE_{II} , until a minimum was achieved for the sum

$$\sum [\ln(\sigma T)_{\text{obs}} - \ln(\sigma T)_{\text{calc}}]^2,$$

where the summation includes all the measured points in the extrinsic and intrinsic temperature regions, $(\sigma T)_{\text{calc}}$ is the calculated σT value using a trial set of the parameters a_I , a_{II} , ΔE_I , and ΔE_{II} , and $(\sigma T)_{\text{obs}}$ is the observed value. The resulting minimum is flat, and the possible presence of local minima demands extra care in interpreting the results. Furthermore, the measured points should also in this case be distributed over a wide temperature range, and one of the exponents should preferably be at least twice the other.^{33,48} The advantage of the computer fit is that all points are included in the calculation and not only the points at the ends of the interval. However, the conductivity curves

shown in Fig. 5 do not consist of only two temperature regions. For the 0.7- and 0.9-GPa runs, a downward deviation of the conductivity curve could be detected at the highest temperatures (region I''). The electrical conductivity in this region at a pressure of 1.0 GPa is shown in Fig. 6. Furthermore, an upward bend of the conductivity curve could be detected in region I'. For all the computer fits $(\sigma T)_{\text{obs}}$ was systematically larger than the $(\sigma T)_{\text{calc}}$ in this region. The results from the computer fits in regions I and II are summarized in Table II. The accuracy of the ΔE values is estimated to be ± 0.1 eV for region I and ± 0.05 eV for region II.

The pressure dependence of the electrical conductivity was studied for the four temperature ranges described above. The activation volume was calculated from Eqs. (6) and (7) using the compressibility⁴¹ 3.27×10^{-11} m²/N and Grüneisen constant⁴⁹ 1.74. The values for $kT\kappa\gamma$ are small compared to the term $kT(\partial \ln R / \partial p)$ and are thus of little importance in this phase. An example of a $\ln(1/R)$ versus pressure plot is shown in Fig. 7. In all these plots a curvature could be detected if the pressure range was sufficiently large. This results in a decreasing activation volume with increasing pressure, as observed earlier.^{50,51} The activation volumes at 0.7 and 0.9 GPa are summarized in Table III for temperatures up to 256°C. The accuracy of the activation volumes in Table III is estimated to be better than ± 2 cm³ mole⁻¹.

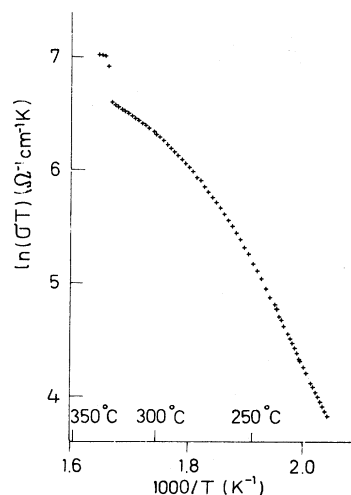


FIG. 6. Temperature dependence of the electrical conductivity of fcc AgI in the high-temperature region at a pressure of 1.0 GPa. The transition to α -AgI is also included.

TABLE II. The results of least-squares fits to the regions I and II for fcc AgI.

Pressure (GPa)	a_I ($\text{K } \Omega^{-1} \text{cm}^{-1}$)	ΔE_I (eV)	a_{II} ($\text{K } \Omega^{-1} \text{cm}^{-1}$)	ΔE_{II} (eV)
0.48	3.2×10^{12}	0.92	2.4×10^3	0.27
0.5	1.4×10^{12}	0.90	1.6×10^3	0.25
0.6	2.8×10^{11}	0.87	0.32×10^3	0.22
0.7	4.1×10^{11}	0.90	0.30×10^3	0.22
0.8	2.3×10^{12}	0.98		
0.9	1.0×10^{11}	0.89	0.11×10^3	0.20

IV. DISCUSSION

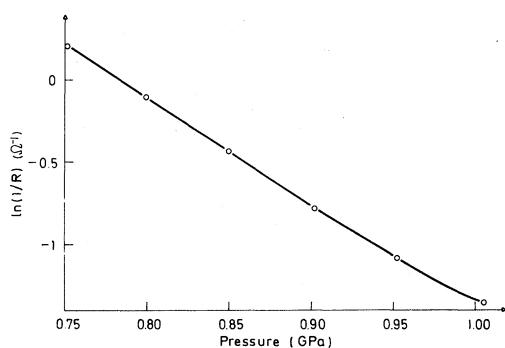
A. α -AgI

The present result for the temperature dependence of the electrical conductivity is in good agreement with earlier data; see Table IV. The results of Tubandt and Lorenz⁶ and Kvist and Josefson⁵² have been recalculated, and the values presented in Table IV are the results of least-squares fits to straight lines in $\ln(\sigma T)$ vs $1/T$ plots for temperatures up to 350°C. Lieser's⁵³ data are presented as activation energies Q calculated from $Q = -k\partial(\ln\sigma)/\partial(1/T)$. The migration enthalpy ΔH_m is obtained from

$$\Delta H_m = Q + kT, \quad (11)$$

which was used for the recalculation in this case. The migration enthalpy calculated from tracer-diffusion measurements,⁵⁴ 0.095 eV, is in good agreement with the calculated values from the electrical conductivity measurements. ΔH_m is thus only slightly larger than the thermal energy kT , which means that the silver ions have to surmount only a very low energy barrier to pass from one tetrahedral site to another.

The electrical conductivity above 350°C was not studied in the present work. Josefson *et al.*⁵⁵ reported a downward bend in the conductivity plot

FIG. 7. $\ln(1/R)$ vs pressure for fcc AgI at 218°C.

for temperatures above about 400°C; i.e., the conductivity was lower than expected from an extrapolation from lower temperatures. They attributed this to the suggested order-disorder transition at 430°C.⁵⁶ The existence of this transition has, however, been doubted by other authors.^{42,47} Josefson *et al.*⁵⁵ also reported a deviation from linearity in the Arrhenius plot of their tracer-diffusion data, but the bend was in this case upward. This meant that for temperatures over 400°C the apparent activation energy increased for diffusion while it decreased for electrical conductivity. Our recalculation of Kvist and Josefson's data⁵² shows, however, that if their conductivity data are plotted as $\ln(\sigma T)$ vs $1/T$ instead of as $\ln\sigma$ vs $1/T$, the bend is also upward for the conductivity. In fact Tubandt and Lorenz's results⁶ at high temperatures show a similar deviation from linearity when plotted in a $\ln(\sigma T)$ vs $1/T$ diagram. We therefore performed a differential scanning calorimetry measurement on AgI, but no indication of an order-disorder transition was found between the first-order transition at 147°C and the melting point at 555°C, even if the AgI was precipitated according to the method of Perrott and Fletcher.³⁶ In contrast to this result in-

TABLE III. Activation volumes for fcc AgI at 0.7 and 0.9 GPa.

	Temperature (°C)	ΔV	
		$p=0.7$ GPa $\text{cm}^3 \text{mole}^{-1}$	$p=0.9$ GPa $\text{cm}^3 \text{mole}^{-1}$
Region II	25	9.4	8.9 ^a
	70	11.6 ^a	10.9 ^a
Region I	158	17.3	16.6
	203	24.2	22.0
Region I'	211		24.4
	218		26.0
	225		23.3
	235		21.5
Region I''	256		15.3

^aFrom Ref. 51.

TABLE IV. Migration enthalpy and the preexponential factor for electrical conductivity measurements in α -AgI for temperatures up to 350°C.

	ΔH_m (eV)	$(\sigma T)_0$ (K Ω^{-1} cm $^{-1}$)
Tubandt and Lorenz (Ref. 6)	0.098	8.2×10^3
Lieser (Ref. 53)	0.097–0.099	
Kvist and Josefson (Ref. 52)	0.102	9.0×10^3
Allen and Lazarus (Ref. 47)	0.10 ± 0.01	
This investigation	0.098 ± 0.001	$(8.0 \pm 0.3) \times 10^3$

dications of changes in the rheological properties,⁵⁷ the thermal expansion,⁴⁶ and in the Raman spectrum^{58–60} have been reported at about 400°C.

A liquidlike model for the mobile silver ions has been suggested to explain the high conductivity in α -AgI (see, e.g., Funke¹). In this model the residence time in a lattice site is shorter than the flight time between different sites. However, the jump-diffusion model has gained support lately.⁶¹ The jump frequency ω can be calculated from

$$\omega = \frac{k\sigma T}{nq^2 a^2 \alpha}, \quad (12)$$

where n equals the number of silver ions per unit volume and the jump distance a is the distance between tetrahedral sites. The jump frequencies in Table V were calculated using the present σT values, the lattice constant of Cava *et al.*,⁸ and the geometrical factor $\alpha = \frac{1}{6}$. The jump-attempt frequency ν can be determined from

$$\omega = \nu \exp(-\Delta H_m/kT + \Delta S_m/k). \quad (13)$$

Since in this case ΔS_m is not known, the attempt frequency can only be estimated if ΔS_m is assumed to be negligible. With the use of this approximation we get $\nu = 5 \times 10^{12}$ s $^{-1}$ at 200°C, which is reasonable since the expected order of magnitude for such a vibration frequency is $10^{12} - 10^{13}$ s $^{-1}$.

Allen and Lazarus⁴⁷ used pressures up to 0.4 GPa to determine the activation volume for α -AgI. Their data are in good agreement with the present data (see Table I), considering the difficulties in

detecting the small changes in resistance induced by the pressure change. Furthermore, Allen and Lazarus used the bulk modulus and Grüneisen constant for RbAg₄I₅ in calculating the migration volume, since no other data were available at that time. The increase in the migration volume with increasing temperature observed by Allen and Lazarus is confirmed in the present investigation. As they pointed out, the migration volume in α -AgI is unusually small. Only few studies have been performed on the pressure dependence of the electrical conductivity in other solid electrolytes. The silver-ion conductor α -RbAg₄I₅ has been shown to have a small negative activation volume $\Delta V = -0.4 \pm 0.2$ cm³ mole $^{-1}$ at room temperature.^{47,62} Radzilowski and Kummer⁶³ investigated the effect of pressure on the electrical conductivity of the ceramic solid electrolyte sodium β -alumina as well as potassium- and lithium-substituted β -alumina. Their results show an electrical conductivity independent of pressure for sodium β -alumina. For potassium-substituted β -alumina the electrical conductivity decreases, while for lithium-substituted β -alumina the electrical conductivity increases with increasing pressure. The activation volumes were not calculated in their paper, but they are expected to be about zero for sodium diffusion, greater than 0 for potassium diffusion, and less than 0 for lithium diffusion. Radzilowski and Kummer explained this in terms of ionic size. The size of the sodium ion makes it possible to pass the saddle point without steric hindrance, while the larger potassium ion will cause lattice dilatation during its passage. The very small lithium ion does not follow the same path as the bigger ions; instead it is attracted towards the walls of the passages. Increasing pressure thus leads to a better fit of the lithium ion to the passages and results in higher conductivity. The measurements of Itoh *et al.*⁶⁴ on sodium β -alumina confirmed that the conductivity is pressure independent up to about 3 GPa but at higher pressures the conductivity decreased. With the use of the arguments

TABLE V. Calculated jump frequencies for α -AgI.

Temperature (°C)	ω (s $^{-1}$)
160	3.8×10^{11}
200	4.7×10^{11}
250	6.0×10^{11}
300	7.2×10^{11}
350	8.5×10^{11}

above this is explained by the diminishing space inside the passages forcing the sodium ions to expand the lattice in passing the saddle point. Thus the low positive migration volume for α -AgI might indicate that the silver ions are somewhat larger than the optimum size for ion transport (cf. Flygare and Huggins⁶⁵). A model that is applicable to molten salts and to solid electrolytes⁶⁶ predicts an activation volume of $0.68 \text{ cm}^3 \text{ mole}^{-1}$ for α -AgI at 200°C , and also that the activation volume should increase with increasing temperature.

B. fcc AgI

The electrical conductivity in the fcc phase is relatively high; at room temperature and a pressure of 0.4 GPa it is even higher than in γ -AgI at normal pressure. Cation Frenkel defects have been shown to dominate in AgCl and AgBr,⁶⁷ and it is thus reasonable to assume that cation Frenkel defects dominate also in the isostructural fcc AgI. The present activation energies in the extrinsic region ΔE_{II} in Table II are in fair agreement with the ones presented by Baranowski *et al.*⁵¹ Furthermore, ΔE_{II} can be compared to the enthalpies for interstitial and vacancy migration of silver ions in AgCl of 0.15 and 0.32 eV (Ref. 68) and in AgBr of 0.20 and 0.33 eV, respectively.⁶⁹ It must be pointed out that the decreasing value of ΔE_{II} with increasing pressure can indicate an electronic contribution to the electrical conductivity at low temperatures. If, however, the electronic contribution is negligible and the same transport mechanism dominates in both region I and II, the formation enthalpy ΔH_f calculated from Eqs. (1) and (3) increases only slightly with increasing pressure from 1.30 to 1.38 eV. This value is comparable to the corresponding values for AgCl, 1.45 eV, and AgBr, 1.13 eV.⁶⁷ Baranowski *et al.*⁵¹ studied the temperature dependence of the electrical conductivity in fcc AgI but only within a limited temperature range, at most 130 K. Shaw⁷⁰ used sound-velocity measurements in fcc AgI to calculate an activation energy at 0.5 GPa. His value for temperatures above about 100°C is 0.4 eV.

The upward curvature in region I' could be caused by several different effects: defect-defect interactions, the influence of another transport mechanism or of another mobile component, or a temperature dependence of the formation or migration enthalpies. In AgCl and AgBr the existence of an upward curvature in the conductivity plot start-

ing at $100\text{--}150^\circ\text{C}$ below the melting point is now well established. A temperature dependence of the formation enthalpy for Frenkel defects has been suggested as a possible explanation.^{67,71-75} Hayes and Boyce⁷⁶ have suggested that the upward bend in the conductivity plot in region I' indicates a slow change in the activation parameters when going from region I to region I''. Thus, according to their arguments, the steep slope in region I' should not be interpreted as due to a high activation energy and a large preexponential factor.

A downward bend in the conductivity plot (region I'') as observed in the present work has not been detected for the other silver halides. The present conductivity curves resemble those of ionic crystals with a gradual transition to a solid electrolyte phase.^{35,77-79} The electrical conductivity in region I'' of fcc AgI is high, about $1 \Omega^{-1} \text{ cm}^{-1}$ at 1.0 GPa, i.e., only somewhat lower than in the α phase, and the apparent activation energy is about 0.3 eV. This shows that the properties in this region are typical of a solid electrolyte rather than of a normal ionic crystal with thermally activated defects, and the apparent activation energy in this region thus corresponds to a migration enthalpy. The temperature of the knee between regions I' and I'' is shown by the dashed line in Fig. 1.

The present measurements of the pressure dependence of the electrical conductivity in fcc AgI confirm the deviation from linearity in the $\ln(1/R)$ versus pressure plots reported by Baranowski *et al.*⁵¹ Their measurements that were performed for pressures up to 2.8 GPa, and for temperatures up to 70°C , gave a decreasing activation volume with increasing pressure. A similar pressure dependence has been reported for the intrinsic temperature range of some alkali halides.^{80,81} Many explanations can be suggested for this effect, and in the present case an onset of electronic conductivity cannot be excluded. The activation volume in the extrinsic temperature range is larger than the migration volume found for other silver halides. The migration volumes for interstitials and vacancies in AgCl (Ref. 68) are $3.2 \text{ cm}^3 \text{ mole}^{-1}$ and $4.7 \text{ cm}^3 \text{ mole}^{-1}$, and in AgBr,⁶⁹ $3.6 \text{ cm}^3 \text{ mole}^{-1}$ and $5.5 \text{ cm}^3 \text{ mole}^{-1}$, respectively. If, however, we assume that the electronic contribution is small and that the same transport mechanism is operative in the extrinsic and intrinsic ranges, the formation volume can be calculated from Eqs. (6) and (7). If the activation volumes at 25 and 158°C (Table III) are used, we get the formation volume $\Delta V_f = 15.4 \text{ cm}^3 \text{ mole}^{-1}$ at 0.9 GPa. This value is close to the

formation volumes for AgCl (Ref. 68) of $16.7 \text{ cm}^3 \text{ mole}^{-1}$ and AgBr (Ref. 69) of $14 \text{ cm}^3 \text{ mole}^{-1}$. The magnitude of the formation volume compared to the molar volume V_m can be used as an indicator of whether Frenkel or Schottky defects dominate in an ionic crystal. It has been shown from experiments and recently also from theoretical calculations that ΔV_f is less than V_m for Frenkel defects and larger than V_m for Schottky defects.⁸²⁻⁸⁵ For fcc AgI, ΔV_f is less than the molar volume²⁷ $33.4 \text{ cm}^3 \text{ mole}^{-1}$, which indicates the dominance of Frenkel defects.

At temperatures corresponding to region I' in fcc AgI, the ΔV values increase up to a maximum of $26.0 \text{ cm}^3 \text{ mole}^{-1}$ (see Table III). This might imply an onset of Schottky disorder at high temperatures, but as mentioned earlier the conduction mechanism in this region is not completely understood. The only other measurement of the pressure dependence of the electrical conductivity in region I' for the silver halides reports a higher activation volume for AgBr in this region than in region I.⁸⁶ Theoretical calculations also indicate an increasing formation volume with increasing temperature for AgCl.⁸⁷

Table III shows that the activation volume decreases rapidly after the maximum, giving a considerably lower value for the activation volume in region I''. The activation volume in this range is probably even lower than the value reported at 256°C , but the determination at these high temperatures is difficult due to the restricted pressure interval; see Fig. 1. The activation volume at the highest temperatures thus seems to be of the order of a migration volume, as expected for a solid electrolyte-like material. Thus there are two solid electrolyte phases in AgI: the α phase and the high-

temperature part of the fcc phase. The main difference between the two is that the iodide sublattice is body-centered cubic for the α phase, while it is face-centered cubic for the fcc phase. The conductivity is somewhat lower in the fcc phase than in the bcc phase and, in fact, most solid electrolytes that have the fcc structure have lower conductivities than those that have the bcc structure.⁵ The high-electrical conductivity, low-activation energy, and low-activation volume in region I'' can be explained by an increasing concentration of cation interstitials in region I', saturating in region I''. An estimate of the difference in disorder between two phases can be obtained from the magnitude of the transition entropy. Such calculations have been performed for the $\beta \leftrightarrow \alpha$ transition in AgI at normal pressure.⁸⁸ The entropy for the fcc $\leftrightarrow \alpha$ transition at 0.74 GPa is $4.4 \text{ J mole}^{-1} \text{ K}^{-1}$ calculated from the transition enthalpy and the transition temperature.²³ The corresponding value for the $\beta/\gamma \leftrightarrow \alpha$ transition at normal pressure²³ is $14.4 \text{ J mole}^{-1} \text{ K}^{-1}$. The lower value of the transition entropy for the fcc $\leftrightarrow \alpha$ transition might indicate a considerable disorder among the silver ions in fcc AgI at high temperatures since the properties of α -AgI have only a slight pressure dependence.

ACKNOWLEDGMENTS

I would like to express my gratitude to Professor A. Lundén, Professor B. Baranowski, and Professor D. Lazarus for many valuable discussions. This work has been supported financially by the Swedish Natural Sciences Research Council and Göteborgs Kungliga Vetenskaps- och Vitterhets-samhälle.

*Present address: Department of Physics, University of Illinois at Urbana-Champaign, Urbana IL 61801.

¹K. Funke, *Prog. Solid State Chem.* **11**, 345 (1976); *Semicond. Insul.* **3**, 351 (1978); *Festkörperprobleme* **20**, 1 (1980).

²K. Shahi, *Phys. Status Solidi A* **41**, 11 (1977).

³A. Hooper, *Contemp. Phys.* **19**, 147 (1978).

⁴S. Geller, *Acc. Chem. Res.* **11**, 87 (1978).

⁵J. B. Boyce and B. A. Huberman, *Phys. Rep.* **51**, 189 (1979).

⁶C. Tubandt and E. Lorenz, *Z. Phys. Chem. (Leipzig)* **87**, 513 (1914).

⁷L. W. Strock, *Z. Phys. Chem. B (Leipzig)* **25**, 441 (1934); **31**, 132 (1936).

⁸R. J. Cava, F. Reidinger, and B. J. Wuench, *Solid State*

Commun. **24**, 411 (1977).

⁹S. Hoshino, T. Sakuma, and Y. Fujii, *Solid State Commun.* **22**, 763 (1977).

¹⁰A. F. Wright and B. E. F. Fender, *J. Phys. C* **10**, 2261 (1977).

¹¹J. B. Boyce, T. M. Hayes, W. Stutius, and J. C. Mikkelsen, Jr., *Phys. Rev. Lett.* **38**, 1362 (1977).

¹²T. M. Hayes, J. B. Boyce, and J. L. Beeby, *J. Phys. C* **11**, 2931 (1978).

¹³J. B. Boyce, T. M. Hayes, and J. C. Mikkelsen, Jr., *Phys. Rev. B* **23**, 2876 (1981).

¹⁴G. Burns, F. H. Dacol, and M. W. Shafer, *Phys. Rev. B* **16**, 1416 (1977).

¹⁵P. Vashishta and A. Rahman, *Phys. Rev. Lett.* **40**, 1337 (1978).

- ¹⁶P. Vashishta and A. Rahman, in *Fast Ion Transport in Solids*, edited by P. Vashishta, J. N. Mundy, and G. K. Shenoy (North-Holland, New York, 1979), p. 527.
- ¹⁷A. J. Majumdar and R. Roy, *J. Phys. Chem.* **63**, 1858 (1959).
- ¹⁸G. Burley, *Am. Mineral.* **48**, 1266 (1963).
- ¹⁹G. Burley, *J. Phys. Chem.* **68**, 1111 (1964).
- ²⁰A. Bienenstock and G. Burley, *J. Phys. Chem. Solids* **24**, 1271 (1963).
- ²¹B. R. Lawn, *Acta Crystallogr.* **17**, 1341 (1964).
- ²²B.-E. Mellander, J. E. Bowling, and B. Baranowski, *Phys. Scr.* **22**, 541 (1980).
- ²³B.-E. Mellander, B. Baranowski, and A. Lundén, *Phys. Rev. B* **23**, 3770 (1981).
- ²⁴T. E. Slykhouse and H. G. Drickamer, *J. Phys. Chem. Solids* **7**, 207 (1958).
- ²⁵B. M. Riggelman and H. G. Drickamer, *J. Chem. Phys.* **38**, 2721 (1963).
- ²⁶A. Van Valkenburg, *J. Res. Natl. Bur. Stand. Sect. A* **68**, 97 (1964).
- ²⁷W. A. Basset and T. Takahashi, *Am. Mineral.* **50**, 1576 (1965).
- ²⁸R. N. Schock and S. Katz, *J. Chem. Phys.* **48**, 2094 (1968).
- ²⁹R. B. Jacobs, *Phys. Rev.* **54**, 325 (1938).
- ³⁰G. J. Piermarini and C. E. Weir, *J. Res. Natl. Bur. Stand. Sect. A* **66**, 325 (1962).
- ³¹A. B. Lidiard, in *Handbuch der Physik*, edited by S. Flügge (Springer, Berlin, 1957), Vol. XX, p. 246.
- ³²P. Süptitz and J. Teltow, *Phys. Status Solidi* **23**, 9 (1967).
- ³³L. W. Barr and A. B. Lidiard, in *Physical Chemistry—An Advanced Treatise*, edited by H. Eyring, D. Henderson, and W. Jost (Academic, New York, 1970), Vol. X, p. 151.
- ³⁴R. G. Fuller, in *Point Defects in Solids*, edited by J. H. Crawford and L. M. Slifkin (Plenum, New York, 1972), Vol. 1, p. 103.
- ³⁵G. A. Samara, *J. Phys. Chem. Solids* **40**, 509 (1979).
- ³⁶C. M. Perrott and N. H. Fletcher, *J. Chem. Phys.* **48**, 2143 (1968).
- ³⁷W. I. Archer and R. D. Armstrong, in *Electrochemistry*, edited by H. R. Thirsk (The Chemical Society, London, 1980), Vol. 7, p. 157.
- ³⁸R. E. Hanneman and H. M. Strong, *J. Appl. Phys.* **36**, 523 (1965); **37**, 612 (1966).
- ³⁹I. C. Getting and G. C. Kennedy, *J. Appl. Phys.* **41**, 4552 (1970).
- ⁴⁰V. M. Cheng, P. C. Allen, and D. Lazarus, *Appl. Phys. Lett.* **26**, 6 (1975).
- ⁴¹G. H. Shaw, *J. Geophys. Res.* **83**, 3519 (1978).
- ⁴²W. Jost, *J. Chem. Phys.* **55**, 4680 (1971).
- ⁴³N. H. Fletcher, *J. Chem. Phys.* **55**, 4681 (1971).
- ⁴⁴J. Nölting and D. Rein, *Z. Phys. Chem. Neue Folge* **66**, 150 (1969).
- ⁴⁵K. H. Lieser, *Z. Phys. Chem. Neue Folge* **5**, 125 (1955).
- ⁴⁶B. Jansson and C.-A. Sjöblom, *Z. Naturforsch. Teil A* **28**, 1539 (1973).
- ⁴⁷P. Allen and D. Lazarus, *Phys. Rev. B* **17**, 1913 (1978).
- ⁴⁸C. S. N. Murthy and P. L. Pratt, *J. Phys. (Paris), Colloq.* **37**, C7-307 (1976).
- ⁴⁹J. Akella, S. N. Vaidya, and G. C. Kennedy, *J. Appl. Phys.* **40**, 2800 (1969).
- ⁵⁰B. Baranowski, A. Lundén, and P. A. Gustavsson, *Phys. Status Solidi A* **31**, K61 (1975).
- ⁵¹B. Baranowski, J. E. Bowling, and A. Lundén, *J. Phys. (Paris) Colloq.* **37**, C7-407 (1976).
- ⁵²A. Kvist and A.-M. Josefson, *Z. Naturforsch. Teil A* **625** (1968).
- ⁵³K. H. Lieser, *Z. Phys. Chem. Neue Folge* **2**, 302 (1956).
- ⁵⁴A. Kvist and R. Tärneberg, *Z. Naturforsch. Teil A* **25**, 257 (1970).
- ⁵⁵A.-M. Josefson, A. Kvist, and R. Tärneberg, in *Atomic Transport in Solids and Liquids*, edited by A. Lodding and T. Lagerwall (*Z. Naturforschung, Tübingen*, 1971), p. 291.
- ⁵⁶C. M. Perrott and N. H. Fletcher, *J. Chem. Phys.* **48**, 2681 (1968); **50**, 2770 (1969); **52**, 3368 (1970).
- ⁵⁷B. Jansson and C.-A. Sjöblom, *Rheol. Acta* **16**, 628 (1977); **20**, 360 (1981).
- ⁵⁸A. Fontana, G. Mariotto, and M. P. Fontana, *Phys. Rev. B* **21**, 1102 (1980).
- ⁵⁹G. Mariotto, A. Fontana, E. Cazzanelli, and M. P. Fontana, *Phys. Status Solidi B* **101**, 341 (1980).
- ⁶⁰G. Mariotto, A. Fontana, E. Cazzanelli, F. Rocca, M. P. Fontana, V. Mazzacurati, and G. Signorelli, *Phys. Rev. B* **23**, 4782 (1981).
- ⁶¹G. Luther and H. Roemer, *Phys. Status Solidi B* **106**, 511 (1981).
- ⁶²K. S. Kim and W. Paik, *J. Chem. Eng. Data* **20**, 356 (1975).
- ⁶³R. H. Radzilowski and J. T. Kummer, *J. Electrochem. Soc.* **118**, 714 (1971).
- ⁶⁴K. Itoh, K. Kondo, A. Sawaoka, and S. Saito, *Jpn. J. Appl. Phys.* **14**, 1237 (1975).
- ⁶⁵W. H. Flygare and R. A. Huggins, *J. Phys. Chem. Solids* **34**, 1199 (1973).
- ⁶⁶B. Baranowski and A. Lundén, in *Fast Ion Transport in Solids*, edited by P. Vashishta, J. N. Mundy, and G. K. Shenoy (North-Holland, New York, 1979), p. 193.
- ⁶⁷J. K. Aboagye and R. J. Friauf, *Phys. Rev. B* **11**, 1654 (1975).
- ⁶⁸A. E. Abey and C. T. Tomizuka, *J. Phys. Chem. Solids* **27**, 1149 (1966).
- ⁶⁹S. Lansiaart and M. Beyeler, *J. Phys. Chem. Solids* **36**, 703 (1975).
- ⁷⁰G. H. Shaw, *J. Phys. Chem. Solids* **41**, 155 (1980).
- ⁷¹A. P. Batra and L. M. Slifkin, *Phys. Rev. B* **12**, 3473 (1975).
- ⁷²A. P. Batra and L. M. Slifkin, *J. Phys. Chem. Solids* **38**, 687 (1977).

- ⁷³C. R. A. Catlow, J. Corish, and P. W. M. Jacobs, *J. Phys. C* **13**, 1977 (1980).
- ⁷⁴P. W. M. Jacobs, J. Corish, and C. R. A. Catlow, *J. Phys. C* **13**, 1977 (1980).
- ⁷⁵P. A. Cardegna and A. L. Laskar, *Phys. Rev. B* **24**, 530 (1981).
- ⁷⁶T. M. Hayes and J. B. Boyce, *Phys. Rev. B* **21**, 2513 (1980).
- ⁷⁷V. M. Carr, A. V. Chadwick, and R. Saghafian, *J. Phys. C* **11**, L637 (1978).
- ⁷⁸J. Oberschmidt and D. Lazarus, *Phys. Rev. B* **21**, 5823 (1980).
- ⁷⁹T. Hibma, *Phys. Rev. B* **15**, 5797 (1977).
- ⁸⁰D. Lazarus, D. N. Yoon, and R. N. Jeffery, *Z. Naturforsch. Teil A* **26**, 56 (1971).
- ⁸¹D. N. Yoon and D. Lazarus, *Phys. Rev. B* **5**, 4935 (1972).
- ⁸²J. Oberschmidt and D. Lazarus, *Phys. Rev. B* **21**, 5813 (1980).
- ⁸³G. A. Samara, *Phys. Rev. B* **22**, 6476 (1980).
- ⁸⁴A. B. Lidiard, *Philos. Mag. A* **43**, 291 (1981).
- ⁸⁵M. J. Gillan, *Philos. Mag. A* **43**, 301 (1981).
- ⁸⁶S. W. Kurnick, *J. Chem. Phys.* **20**, 218 (1952).
- ⁸⁷C. R. A. Catlow, J. Corish, P. W. M. Jacobs, and A. B. Lidiard, *J. Phys. C* **14**, L121 (1981).
- ⁸⁸H. U. Beyeler and S. Strässler, *Phys. Rev. B* **20**, 1980 (1979).